Resonant Enhancement of Tunneling Magnetoresistance in Double-Barrier Magnetic Heterostructures

A. G. Petukhov,[1,2] A. N. Chantis,[2] and D. O. Demchenko[2]

[1]*Center for Computational Materials Science, Naval Research Laboratory, Washington, D.C. 20375*
[2]*Physics Department, South Dakota School of Mines and Technology, Rapid City, South Dakota 57701*

(Received 22 April 2002; published 20 August 2002)

We show that spin-dependent resonant tunneling can dramatically enhance tunneling magnetoresistance. We consider double-barrier structures comprising a semiconductor quantum well between two insulating barriers and two ferromagnetic electrodes. By tuning the width of the quantum well, the lowest resonant level can be moved into the energy interval where the density of states for minority spins is zero. This leads to a great enhancement of the magnetoresistance, which exhibits a strong maximum as a function of the quantum well width. We demonstrate that magnetoresistance exceeding 800% is achievable in GaMnAs/AlAs/GaAs/AlAs/GaMnAs double-barrier structures.

DOI: 10.1103/PhysRevLett.89.107205 PACS numbers: 75.70.Pa, 73.40.Gk, 75.50.Pp, 85.75.Mm

Spin-dependent tunneling in solids has been a subject of great interest since the discovery of tunneling magnetoresistance (TMR) in magnetic tunnel junctions (MTJ) [1]. Recent advances in heteroepiatxial growth of GaMnAs [2] and other III-V dilute magnetic semiconductors (DMS) [3,4] sparked even more interest due to the scientific and technological applications offered by all-semiconductor magnetic devices. Among different types of spin-dependent transport in magnetic heterostructures, spin-dependent resonant tunneling has been relatively unexplored theoretically, despite the fact that spin-dependent resonant tunneling devices (spin-RTDs) have been fabricated. The experiments on spin-RTDs revealed a remarkable interplay of magnetism, spin-orbit coupling, and quantum confinement, resulting in pronounced spin selectivity that can be controlled by an external bias or magnetic field [5,6]. In this Letter we demonstrate that the spin-dependent resonant tunneling in double-barrier magnetic junctions can dramatically enhance magnetoresistance as compared with traditional single barrier junctions.

Using a one-band spin-polarized model [7] as a generic example, we will show that at certain conditions the spin-RTD may act as an almost ideal spin valve, allowing for the resonant tunneling in the majority spin channel only, and only for the parallel (ferromagnetic) alignment of the magnetizations in the emitter and collector. Even though one-band models of spin-RTDs have been considered in the literature [8,9],the resonant spin-valve effect described below has never been discussed, to the best of our knowledge. We will consider small biases, where only the electrons at the Fermi surface contribute to the tunneling current, and will take into account elastic processes only. The double-barrier structure in question is shown in Fig. 1, where w and L are the barrier and the well widths, respectively, and Δ_{ex} is the exchange splitting. As usual, we will compare configurations with the parallel (ferromagnetic, F) and the antiparallel (antiferromagnetic, AF) alignments of the magnetizations in the leads, and define tunneling magnetoresistance as $\mathrm{TMR} = (G_{\mathrm{F}}/G_{\mathrm{AF}} - 1) \cdot 100\%$, where $G_{\mathrm{F(AF)}}$ are the linear-response conductances [7,10] for the F and AF configurations, respectively. Figure 1 presents the situation where the geometric parameters of the double-barrier heterostructure (DBH) are tuned in such a way that the resonant level E_R in the well falls into the energy interval $0 < E_R < \Delta_{ex}/2$, where the density of states for the minority spins in the emitter is 0. The resonant conditions for the F configuration (Figs. 1(a) and 1(b)) are

$$\mp \frac{\Delta_{ex}}{2} + \frac{\hbar^2}{2m^*} k_{z,L}^2 = \mp \frac{\Delta_{ex}}{2} + \frac{\hbar^2}{2m^*} k_{z,R}^2 = E_R, \quad (1)$$

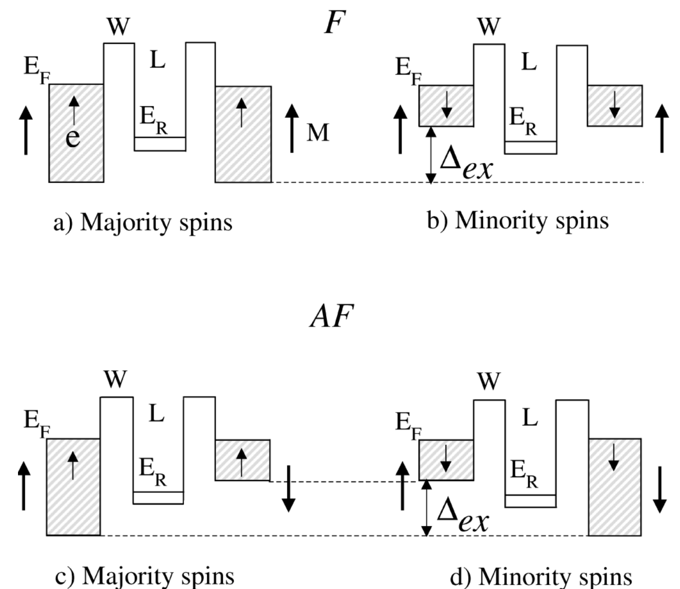

FIG. 1. Schematic flat-band diagrams illustrating the resonant spin-valve effect

 © 2002 The American Physical Society

where signs “−” and “+” correspond to the majority and minority spin channels, respectively. The similar conditions for the AF configuration (Fig. 1(c) and 1(d)) read

$$\mp \frac{\Delta_{ex}}{2} + \frac{\hbar^2}{2m^*} k_{z,L}^2 = \pm \frac{\Delta_{ex}}{2} + \frac{\hbar^2}{2m^*} k_{z,R}^2 = E_R. \quad (2)$$

Here m^* is the effective mass, $k_{z,L(R)}$ is the wave-vector component in the direction of the current in the emitter (collector), $E_R = E_F - \hbar^2 k_\parallel^2/2m^*$, $\vec{k}_\parallel$ is the inplane wave-vector component (assumed to be conserved), and E_F is Fermi energy. The resonant level contributes to the conductance if these conditions are satisfied along with the obvious requirement $k_z^2 > 0$. Analysis of Eqs. (1) and (2) shows that in the case when $0 < E_R < \Delta_{ex}/2$ the resonant level contributes to the conductance only through the majority channel in the F configuration. If this is the only resonant level under the Fermi level of the emitter, the conductance in the AF configuration is purely nonresonant and the system works as an almost ideal spin valve even though the ferromagnetic leads are not half-metallic. Another look at this effect is shown in the inset in Fig. 2, which is a graphical representation of Eqs. (1) and (2). The Fermi circle corresponding to the resonant level lies between the majority and minority Fermi spheres. Thus the lateral momentum conservation will allow for resonant tunneling in the majority channel only.

To further illustrate our point we use the Breit-Wigner formula (i.e., the Lorentzian approximation) for the transmission coefficient in the vicinity of the resonance:

$$T_\sigma^\alpha(\vec{k}_\parallel, E) = T_{\sigma,NR}^\alpha + T_R \cdot \delta_{\sigma\uparrow} \cdot \delta_{\alpha,\mathrm{F}}, \quad (3)$$

where $T_{\sigma,NR}^\alpha$ describes nonresonant tunneling in the spin channel σ for configuration $\alpha = \mathrm{F(AF)}$, and

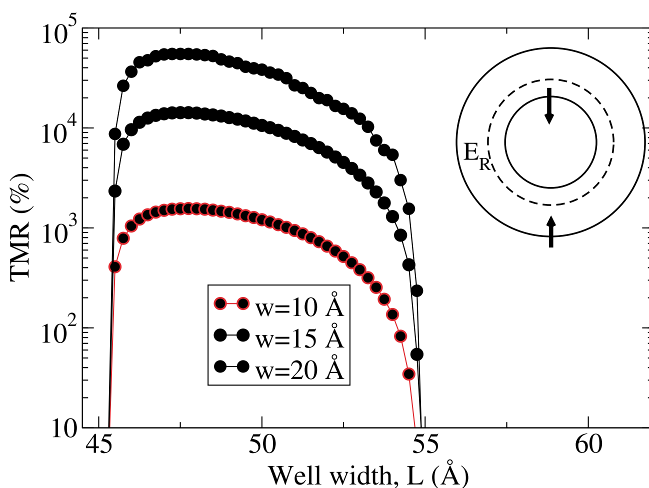

FIG. 2 (color online). TMR of the one-band spin-RTD as a function of the quantum-well width. Inset: Fermi surfaces in the emitter (solid lines) and quantum well (dashed line) corresponding to the maximum TMR.

$$T_R(\vec{k}_\parallel, E) = \frac{\Gamma^2}{(E - E_R - \hbar^2 k_\parallel^2/2m^*)^2 + \Gamma^2} \quad (4)$$

is the resonant part of the transmission coefficient and $\hbar/\Gamma$ is the elastic lifetime of an electron in the well. The conductance at zero-temperature can be calculated by the Landauer’s formula [7,10]:

$$G = \frac{e^2 S}{(2\pi^3)\hbar} \int d^2 k_\parallel T(\vec{k}_\parallel, E_\mathrm{F}), \quad (5)$$

where S is the cross-sectional area of the device. Substituting Eqs. (3) and (4) into Eq. (5) we obtain

$$G_\alpha = \frac{e^2 S}{4\pi\hbar} \left[\frac{k_F}{4\pi w} A_\alpha \exp(-4k_\mathrm{F} w) + \frac{m^*}{\hbar^2} \Gamma \delta_{\alpha,F} \right], \quad (6)$$

where k_F is the Fermi wave vector, and w is width of the barrier. The prefactor A_α depends on the relative directions of the magnetizations. The first term describes the nonresonant part of the conductance [7,11]. It decays exponentially with the barrier width w. The second (resonant) term does not contain the factor $\exp(-4k_\mathrm{F}w)$. As a result, the magnetoresistance grows exponentially with the barrier width:

$$\mathrm{TMR} = (\mathrm{TMR})_{NR} + \Gamma \exp(4k_\mathrm{F} w)/E_\mathrm{AF}, \quad (7)$$

where the last term describes resonant enhancement of TMR, and E_AF is a constant with the units of energy. Formula (7) has no resemblance with the Julliere’s formula [1]. It shows that TMR can be made exponentially large by tuning the parameters of the nonmagnetic part of the junction rather than the spin polarizations in the leads.

To corroborate the qualitative conclusion based on the Breit-Wigner formula we calculate the conductance with the exact transmission coefficient for the one-band model. The results are shown in Fig. 2. They correspond to $E_\mathrm{F} =$ 80 meV, $\Delta_{ex} = 50$ meV, and $m^* = 0.5m_0$. TMR as a function of the quantum-well width L displays a very pronounced maximum which can reach up to $10^4\%$. The maximum can be explained as follows: the sharp increase of the magnetoresistance is due to the fact that the lowest resonant level in the well falls into the interval $0 < E_R < \Delta_{ex}/2$. As soon as the second resonant level becomes lower than the Fermi energy, both the F and AF conductances contain resonant parts, plus the lowest resonant level becomes narrower and does not play a crucial role anymore. As as result, TMR starts decreasing.

The one-band model provides good qualitative insight into the problem, however it cannot be used for a quantitative description of tunneling in III-V DMS where the tunneling carriers are holes and the complexity of the valence band and the spin-orbit coupling play very important roles. Below we present more realistic calculations of a GaMnAs-based DBH, taking these factors into account. GaMnAs is a p-type ferromagnetic DMS with maximum Curie temperature 110 K. GaMnAs DBH were fabricated

and giant tunneling magnetoresistance was observed in trilayer [12] and double-barrier structures [13]. Spin-dependent resonant tunneling in GaMnAs-based RTDs was also observed [6].

Our calculation of the transmission coefficient is based on a multiband transfer matrix technique [14]. We start from the hole Hamiltonian of a magnetic semiconductor

$$H_h = \frac{1}{2}(H_h^{\uparrow} + H_h^{\downarrow})I + \frac{1}{2}(H_h^{\uparrow} - H_h^{\downarrow})(\vec{\sigma} \cdot \hat{n}) + \frac{1}{2}\lambda_{so}\vec{\sigma}\vec{L}, \tag{8}$$

where I is 2×2 unit matrix, $\vec{\sigma} \equiv (\sigma_x, \sigma_y, \sigma_z)$, σ_α are the Pauli matrices, $\hat{n}$ is the unit vector in the direction of magnetization, λ_{so}-spin-orbit coupling constant, and

$$H_h^\sigma = -\gamma_0^\sigma - (\gamma_1^\sigma + 4\gamma_2^\sigma)k^2 + 6\gamma_2^\sigma \sum_\alpha L_\alpha^2 k_\alpha^2 + 6\gamma_3^\sigma \sum_{\alpha \neq \beta} (L_\alpha L_\beta + L_\beta L_\alpha) k_\alpha k_\beta, \tag{9}$$

where $\alpha = \{x, y, z\}$, L_α are $l = 1$ angular momentum operators, and γ_i^σ are Luttinger parameters. The parameters γ_0^σ, describing the exchange splitting at $\vec{k} = 0$, can be expressed through the constant β of the $p - d$ exchange interaction: $\gamma_0^{\uparrow} - \gamma_0^{\downarrow} \equiv 3\Delta_{ex} = \frac{5}{2}\beta N_0 x$, where Δ_{ex} is the exchange splitting of the light holes (LH) at the Γ-point, N_0 is the number of cations per unit volume in GaMnAs, and x is Mn concentration. The constant $\beta N_0 \simeq -1.2$ eV according to Dietl *et al.* [2] which leads to $\Delta_{ex} = 50$ meV at $T = 0$ and $x = 0.05$. Neglecting the spin dependence of $\gamma_{i\neq 0}^\sigma$ will reduce our hole Hamiltonian H_h to a more conventional "Kohn-Luttinger + exchange" mean-field Hamiltonian used for dilute magnetic semiconductors (e.g., [2]). In the nonmagnetic GaAs and AlAs regions we used the standard Kohn-Luttinger hole Hamiltonian [14].

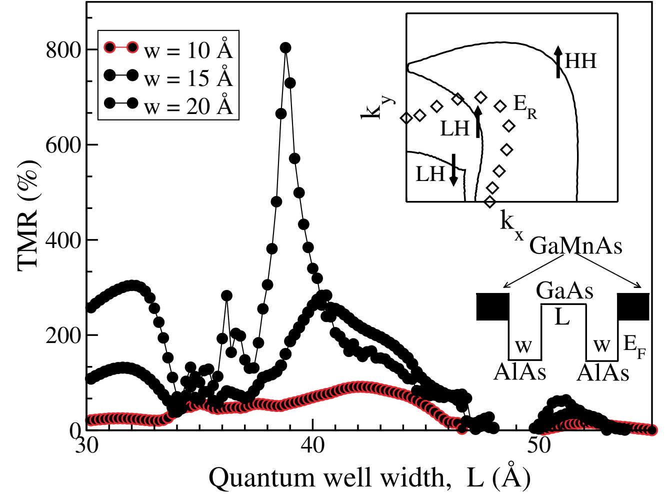

FIG. 3 (color online). TMR of GaMnAs/AlAs/GaAs-based spin-RTDs as a function of the quantum-well width. Upper inset: Fermi surfaces in the emitter (solid) line and quantum well (diamonds) corresponding to the maximum TMR. Lower inset: schematic band diagram.

We represent the device as a stack of two-dimensional flat-band interior layers with thickness w_n and potentials V_n, starting at $z_0 = 0$ and ending at $z_N = L_d$ (where L_d is the length of the device), plus two semi-infinite leads. Below we will use $N = 3$ [see Fig. 3 (inset)]. The thickness of the n_{th} interior layer is $w_n = z_n - z_0$. The 0_{th} and $(N+1)_{th}$ layers are the semi-infinite emitter ($z < 0$) and collector ($z > L_d$). Substituting $k_z \to -i\hbar\partial/\partial z$ one can solve the Schrödinger equation in the n_{th} flat-band region:

$$\Psi_n(z) = \sum_{\alpha=1}^{n_b} [A_{n,\alpha}^+ v(k_{n,\alpha}) \exp(ik_{n,\alpha}z) + A_{n,\alpha}^- v(-k_{n,\alpha}) \exp(-ik_{n,\alpha}z)], \tag{10}$$

where n_b is the number of bands, $n_b = 6$ for the Hamiltonian (8), and $k_{n\alpha}$ are the generalized complex eigenvalues of k_z in the n_{th} flat-band region. These eigenvalues, which always occur in pairs $\pm k_{n\alpha}$, and corresponding eigenvectors $v(\pm k_{n\alpha})$ can be found from the equation

$$[H_n^{(2)}(\vec{k}_\parallel)k_n^2 + H_n^{(1)}(\vec{k}_\parallel)k_n + H_n^{(0)}(\vec{k}_\parallel) - E]v = 0, \tag{11}$$

where we took advantage of the fact that the Hamiltonian (8) can be represented as a quadratic function of k_z with "coefficients" $H_n^{(i)}$ that are $n_b \times n_b$ matrices. The matrices $H_n^{(0)}$ contain a constant energy shift (barrier height) of -0.55 eV in the AlAs regions [15]. Equation (11) can be reduced to the regular eigenvalue problem for a non-Hermitian matrix [16,17]. In order to formulate boundary conditions in the matrix form we need to define the current operator [16] as $J_z(k_{n\alpha}) = [2H_n^{(2)}k_{n\alpha} + H_n^{(1)}]/\hbar$.

The set of the coefficients $A_{n\alpha}^+$ corresponds to the solutions that are either traveling waves carrying the probability current from left to right or evanescent waves exponentially decaying to the right (i.e., in the positive direction of z). The corresponding eigenvalues $k_{n\alpha}$ satisfy the following conditions

$$k_{n\alpha} \in \{A^+\}: \begin{array}{lll} \text{if} & \text{Im}(k_{n\alpha}) = 0 & \text{and } j_{n\alpha} > 0; \\ \text{or} & \text{Im}(k_{n\alpha}) > 0, & \end{array} \tag{12}$$

where $j_{n\alpha} = \text{Re}[v^+(k_{n\alpha})J_{nz}(k_{n\alpha})v(k_{n\alpha})]$ is the expectation value of the probability current. Respectively, the set $\{A^-\}$ contains all "right-to-left" eigenvalues $-k_{n\alpha}$. The matching conditions at the interface z_n ($n = 0, .., N$), corresponding to the continuity of the wave function and the current can be expressed in matrix form as follows:

$$\mu_n f^n(z_n)A_n = \mu_{n+1}f^{n+1}(z_n)A_{n+1}, \tag{13}$$

where μ_n is the matrix comprised of $2n_b$ eigenvectors $v(k_{n\alpha})$

$$\mu_n = \begin{bmatrix} . & v(k_{n\alpha}) & . & v(-k_{n\alpha}) & . \\ . & J_z(k_{n\alpha})v(k_{n\alpha}) & . & J_z(-k_{n\alpha})v(-k_{n\alpha}) & . \end{bmatrix}, \tag{14}$$

and $f^n_{\alpha\beta}(z) = \exp(ik_{n\alpha}z)\delta_{\alpha\beta}$.

We adopt the following convention for enumeration of the lead layers and all related quantities: $0 \equiv L$ (emitter) and $N + 1 \equiv R$ (collector). The system of linear Eqs. (13) can be solved as

$$\begin{pmatrix} A_L^+ \\ A_L^- \end{pmatrix} = M\begin{pmatrix} A_R^+ \\ A_R^- \end{pmatrix} \equiv \begin{pmatrix} M_+ & M_{+-} \\ M_{-+} & M_- \end{pmatrix}\begin{pmatrix} A_R^+ \\ A_R^- \end{pmatrix}, \tag{15}$$

where the $2n_b \times 2n_b$ transfer matrix

$$M = \mu_L^{-1}\left[\prod_{n=1}^{N} \mu_n f^n(-w_n)\mu_n^{-1}\right]\mu_R f^{N+1}(z_N)$$

is partitioned according to the criteria (12) in the emitter (L) and collector (R). The boundary condition $A_R^- = 0$ defines the transmission matrix $t_{\alpha\beta}$ in terms of the $n_b \times n_b$ matrix M_+ as

$$t_{\alpha\beta} = \begin{cases} \sqrt{j_{R\beta}/j_{L\alpha}}(M_+)^{-1}_{\beta\alpha}, & \text{if } j_{R\beta(L\alpha)} > 0, \\ & \text{and } \mathrm{Im}k_{R\beta(L\alpha)} = 0, \\ 0, & \text{otherwise}, \end{cases} \tag{16}$$

and the transmission coefficient entering Eq. (5) can be calculated in a usual way [10,18] as $T(\vec{k}_\parallel, E) = Tr(t^\dagger t)$.

Figure 3 shows zero-temperature TMR in GaMnAs-based DBH as a function of the quantum-well width for the inplane magnetization $\vec{M} \parallel [100]$, Fermi energy $E_F = 150$ meV, and $\Delta_{ex} = 50$ meV [2]. These parameters correspond to 5% (1.1×10^{21} cm^{-3}) Mn and 1×10^{20} cm^{-3} hole concentrations, respectively [2]. TMR displays a sharp maximum of ~800% at the well width ~40 Å and barrier width ~20 Å. Even though the value of TMR is not as large as in the one-band case it is still extremely high. The reason for the reduction of TMR (as compared to the one-band case, Fig. 2) is the spin-orbit coupling. Namely, as we see from the inset to Fig. 3 the minority heavy hole (HH) band is empty. As a result, we have only three (rather than four) Fermi surfaces in GaMnAs (see Fig. 3, inset). In this situation one would expect zero transmission coefficient and conductance in the HH channel for antiparallel alignment of the magnetizations. However, due to the spin-orbit coupling, this (spin-flip) transmission is not zero for both HH and LH channels. In fact, it is rather significant especially when $\vec{k}$ is perpendiculr to the magnetization. The suppression of the spin-flip processes involving LH states in the region where the Fermi surface of the quantum well lies in between LH and HH Fermi surfaces ensures, nonetheless, strong enhancement of TMR which depends exponentially on the barrier width. Another important observation is related to the orientation of the magnetization with respect to the interface. We did not find any enhancement of TMR for the magnetizations perpendicular to the layers. This is a direct consequence of the strong anisotropy of the hole Fermi surface in GaMnAs [2].

The predicted value of the zero-temperature magnetoresistance for the one-band model is enormous (~ 10^4%, see Fig. 2). For more realistic multiband calculations with the spin-orbit interaction taken into account, the predicted value of TMR is smaller, but still very large (~ 800%). Because of this fact we expect that the strong spin-valve effect can be observed experimentally in double-barrier magnetic heterostructures. A promising candidate would be a structure based on GaMnN, where both higher Curie temperature and smaller spin-orbit coupling are expected [2].

The work is supported by NSF Grant No. DMR-0071823 and by NRL through the ASEE-NAVY Sabbatical leave program. We are grateful to Igor Mazin and Steve Erwin for fruitful discussions.

[1] M. Julliere, Phys. Lett. **54A**, 225 (1975).
[2] T. Dietl, H. Ohno, F. Matsukura, J. Cibert, and D. Ferrand, Science **287**, 1019 (2000).
[3] M. E. Overberg *et al.*, Appl. Phys. Lett. **79**, 3128 (2001).
[4] M. E. Overberg *et al.*, Appl. Phys. Lett. **79**, 1312 (2001).
[5] D. E. Brehmer *et al.*, Appl. Phys. Lett. **67**, 1268 (1995).
[6] H. Ohno *et al.*, Appl. Phys. Lett. **73**, 363 (1998).
[7] J. C. Slonczewski, Phys. Rev. B **39**, 6995 (1989).
[8] X. Zhang, B. Li, G. Sun, and F. Pu, Phys. Rev. B **56**, 5484 (1997).
[9] A. M. Bratkovsky, Phys. Rev. B **56**, 2344 (1997).
[10] S. Datta, *Electronic Transport in Mesoscopic Systems* (Cambridge University Press, Cambridge, United Kingdom, 1995).
[11] J. Mathon, Phys. Rev. B **56**, 11 810 (1997).
[12] M. Tanaka and Y. Higo, Phys. Rev. Lett. **87**, 026602 (2001).
[13] T. Hayashi, M. Tanaka, and A. Asamitsu, J. Appl. Phys. **87**, 4673 (2000).
[14] C. Y. Chao and S. L. Chuang, Phys. Rev. B **43**, 7027 (1991).
[15] R. Wessel and M. Altarelli, Phys. Rev. B **39**, 12 802 (1989).
[16] Y. X. Liu, D. Z.-Y. Ting, and T. C. McGill, Phys. Rev. B **54**, 5675 (1996).
[17] J. H. Wilkinson, *The Algebraic Eigenvalue Problem* (Oxford University Press, Oxford, United Kingdom, 1965).
[18] C. W. J. Beenakker, Rev. Mod. Phys. **69**, 731 (1997).